

## Introduction

Efforts to understand the fundamental origins of scintillator nonproportionality in order to discover better performing scintillator materials are intensive in the last decade. The transport of the electrons in scintillators after being induced by incident  $\gamma$ -ray can be sub-divided into the hot electron stage with energy range up to one  $E_g$  above conduction band minimum (CBM) and the thermalized electron stage with energy right at CBM. Our nonlinear quenching and diffusion model of thermalized carriers made quite good prediction between the nonproportionality and effective diffusion coefficient ( $D_{eff}$ ) of oxides, while it left some ambiguity to both monovalent and multivalent halide materials. [1] A common similarity for almost all these halide materials is that they have been suggested or proved to have self-trapped holes on a time scale of  $\sim 1$  ps by experiment and/or theoretical approaches, hence we focus mainly on their electron transport. Monte-Carlo modeling for hot electrons losing their energy mainly by scattering with optical phonons has been done for several halide materials in Ref. [2] they concluded that optical phonon frequency is the key factor controlling the electron thermalization time and hence electron transport length. Velocity calculated from a free electron model is used in their simulations to decide the step length. However, it is demonstrated in this work that the inclusion of full band structure significantly improves the result of electron transport velocity with respect to the prediction of free electron model.

## What is nonproportionality?

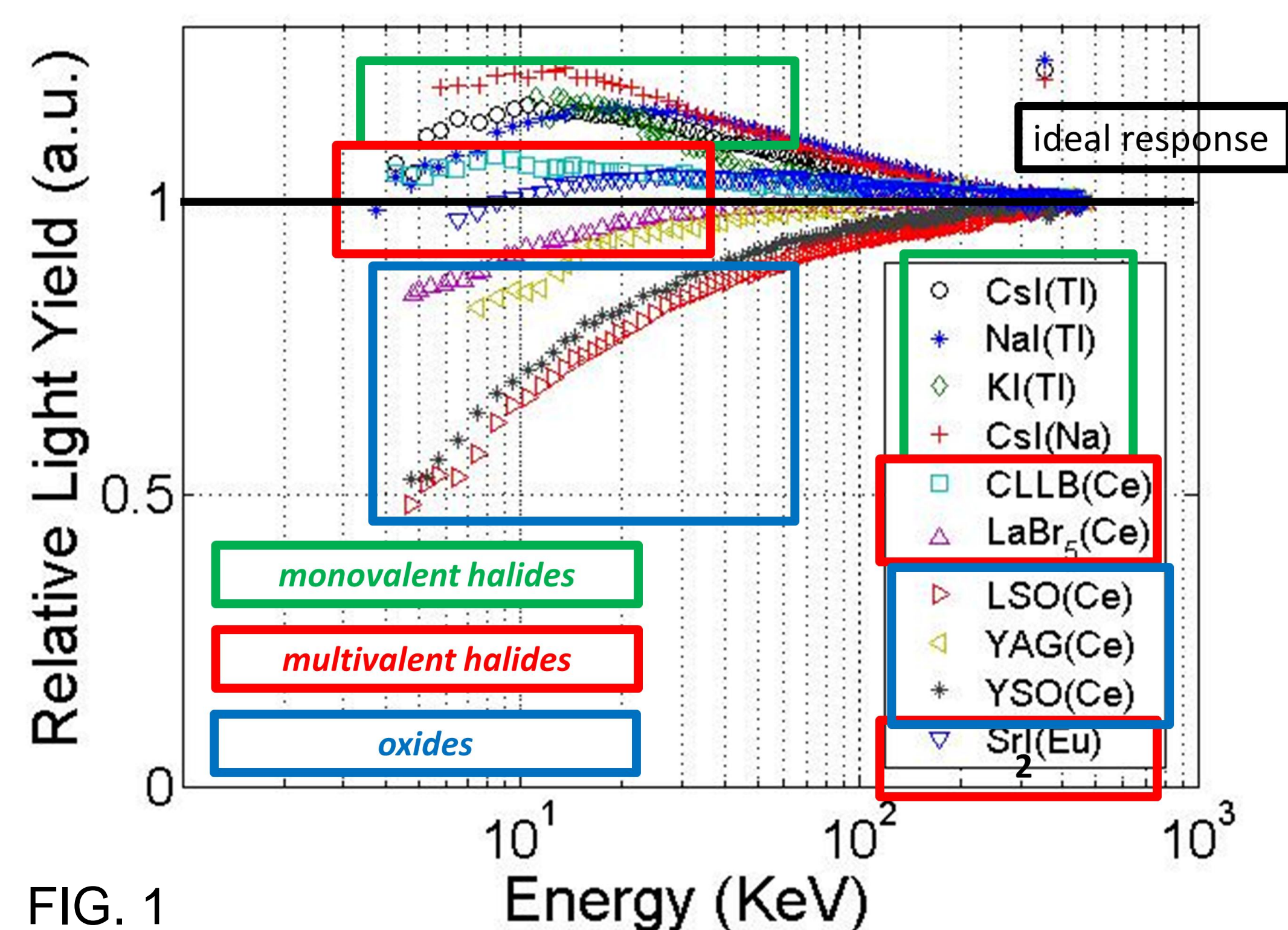


FIG. 1 SLYNCI (Scintillator Light Yield Nonproportionality Compton Instrument) electron light yield, Lawrence Berkeley National Lab & Lawrence Livermore National Laboratory. The response of scintillator materials can be grouped by their host structures.

## The transport & nonlinear quenching model

Our transport & nonlinear quenching model successfully describes the nonproportionality of materials over their effective diffusion coefficient on a large scale of 8 orders of magnitude. However, it left some ambiguity to hole-self trapping halide materials.

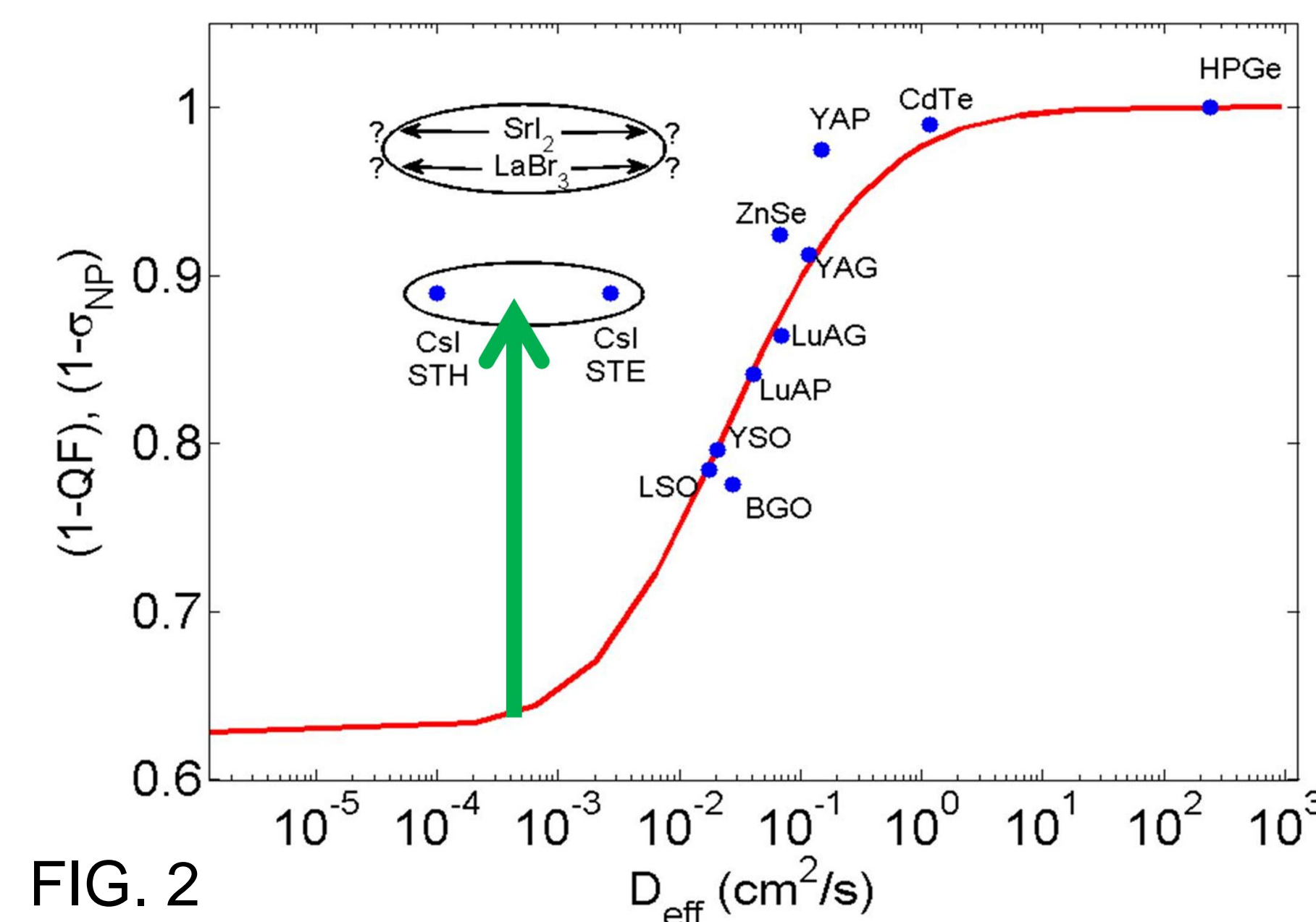


FIG. 2 Diffusion model in Ref. [1], oxides and semiconductors fall on the theoretical curve perfectly. The halides response better than the description of this model itself. The differences between monovalent and multivalent halides, self-trapping and non self-trapping materials are also beyond the prediction ability.

Table I The band gap, refraction index, band mass, quenching, optical phonon frequency for NaI and SrI<sub>2</sub> are listed, we can see that they are very similar in many ways, so what made their response so different?

	NaI	SrI <sub>2</sub>
$E_{gap}$ (eV)	5.8	5.5
$n$	1.85	2.05
$m_e^*$ ( $\Gamma$ )	0.29	0.29
$m_h^*$ ( $\Gamma$ )	2.40	6.36 (0.62)
self-trap?	STH, STE	STH, STE
K-dip quench @ 0.2 keV	35%	38%
z-scan quench @ $1.6 \times 10^{20}$ eh/cm <sup>3</sup>	50%	39%
$\hbar\omega_{LO}$ (eV)	0.023	0.015

Table I

## Calculations of group velocity

The electronic structures are calculated from DFT using the Vienna Ab-initio Simulation Package (VASP) with projector augmented waves (PAW) pseudopotentials and exchange-correlation functionals parameterized by Perdew-Burke-Ernzerhof (PBE) with generalized gradient approximation (GGA). For the Lanthanum compounds, we use DFT+U technique to the La (4f) states to correct their position relative to the La (5d) states. [3] We choose  $U_{eff} = 10.5$  eV in our calculations to reproduce experimental observations. We use  $\Gamma$ -centered Monkhorst-Pack generated kmesh grids to sample the Brillouin zone and average over it to get the group velocities.

$$g(E) = \frac{2}{(2\pi)^3} \sum_n \int_{BZ} \delta(E - E_n(\mathbf{k})) d^3\mathbf{k}$$

$$v_s^2(E)g(E) = \frac{2}{(2\pi)^3} \sum_n \int_{BZ} v_n^2(\mathbf{k}) \delta(E - E_n(\mathbf{k})) d^3\mathbf{k}$$

$$v_n(\mathbf{k}) = (1/\hbar) \nabla_{\mathbf{k}} E_n(\mathbf{k})$$

where  $n$  is the band index, and the factor 2 accounts for the spin degeneracy. [4]

We also calculated the electron band mass to compare the group velocity with the free electron model.

$$v_{FEM} = \sqrt{\frac{2E_e^{kin}}{m_e}}$$

$$m_a = \frac{1}{\hbar^2} \frac{1}{N} \left( \sum_i \frac{\partial^2 E_i}{\partial k_\alpha^2} \right)^{-1}$$

where  $i$  runs all the degenerate bands and optima of CBM.

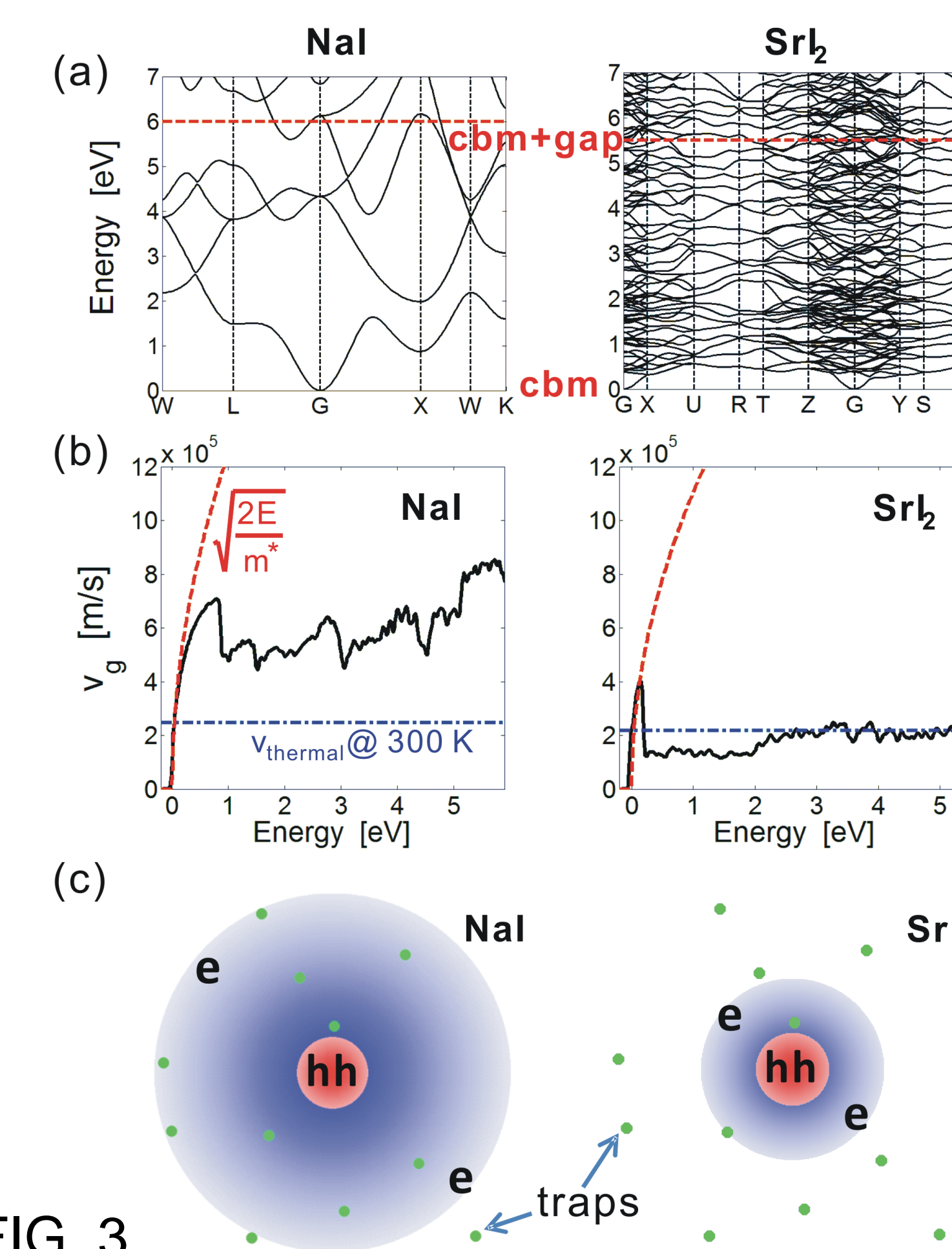


FIG. 3 Comparison in NaI and SrI<sub>2</sub> of (a) conduction band structure, (b) group velocity distribution vs. energy, and (c) schematic representation of electron track cross sections in halides with self-trapped holes at the core, and thermalization range of hot electrons represented by the larger radial distributions.

## Scintillator “decision tree”

To conclude, we propose a broadly applicable model of scintillator nonproportionality depending on optical phonon frequency, thermalized band edge mobilities, group velocity in the upper conduction bands, and occurrence of hole self-trapping or not.

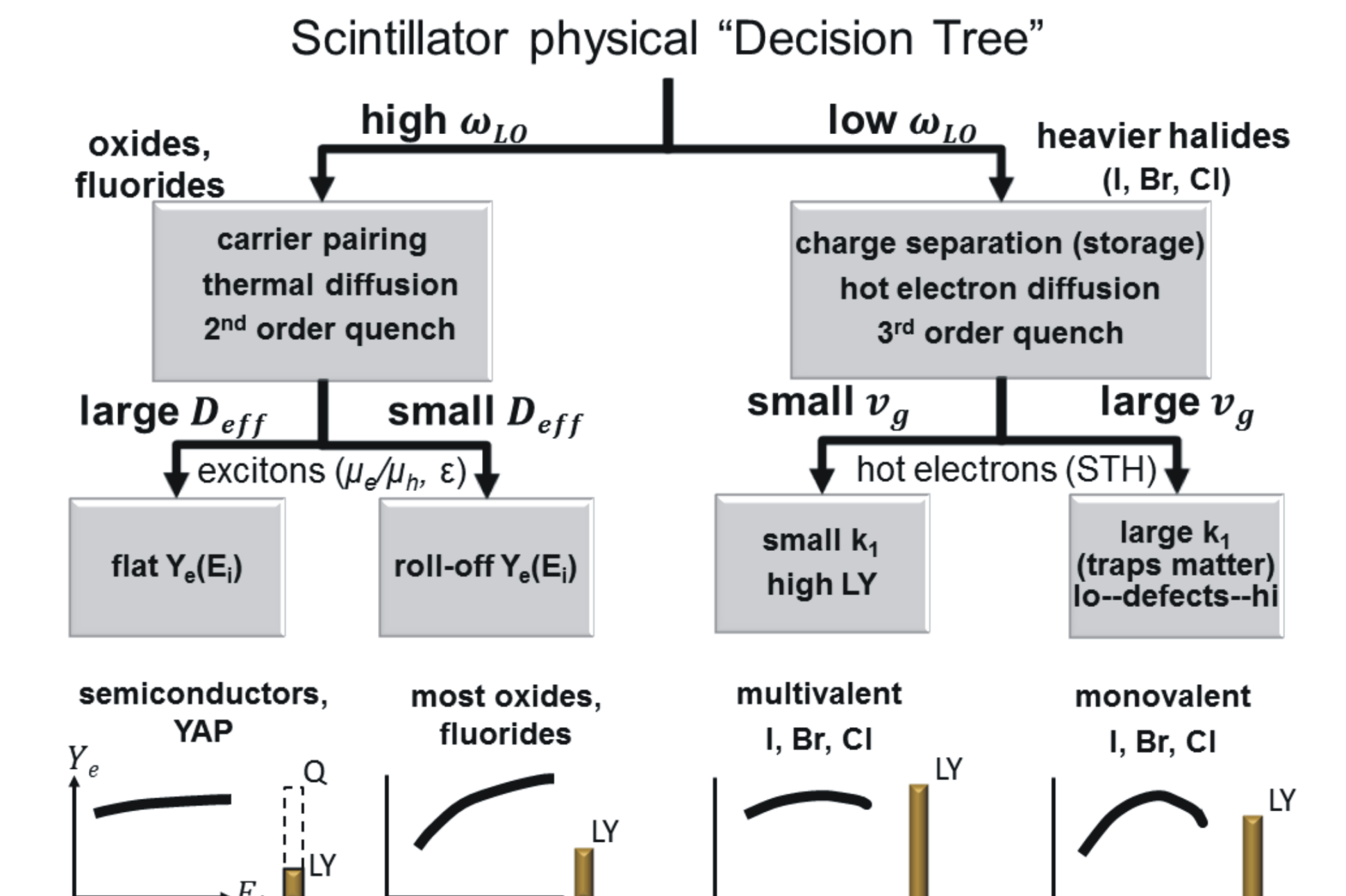


FIG. 2. Illustration of how classes of general behavior in electron energy response and light yield (or charge Q in semiconductors) as depicted along the bottom can result from physical parameter values.  $\hbar\omega_{LO}$  decides electron thermalization rate: fast to the left with thermalized diffusion in oxides and fluorides versus slow to the right with hot free carriers in the heavier halides. Subsequent branching in the thermalized half is governed by band-edge diffusion coefficient  $D_{eff}$  as shown previously in Ref. [1]. The non-thermalized half is controlled by hot-electron velocity and range depending on host structure of the heavier halides (multivalent versus monovalent compounds).

We acknowledge support from the National Nuclear Security Administration, Office of Defense Nuclear Nonproliferation, Office of Nonproliferation Research and Development (NA-22) of the U. S. Department of Energy under Contracts DE-NA0001012 and DE-AC02-05CH11231.

## References

- [1] Qi Li, Joel Q. Grim, R. T. Williams, G. A. Bizarri, and W. W. Moses, *J. Appl. Phys.* **109**, 123716 (2011).
- [2] Z. Wang, Y. Xie, G. Fei, and S. Kerisit, *J. Appl. Phys.*, in press (2012).
- [3] W. Setyawan, R. M. Gaume, R. S. Feigelson, S. Curtarolo, *IEEE Trans. Nucl. Sci.* **56**, 2989 (2009).
- [4] G. Elena. R. Susanna, and R. Massimo, *Physical Review B*, **66**, 195205 (2002).